Available online at www.sciencedirect.com
ScienceDirect
Journal of the European Ceramic Society 32 (2012) 1457–1462
www.elsevier.com/locate/jeurceramsoc

Aluminum diboride synthesis from elemental powders by mechanical alloying and annealing

Duygu Ağaoğulları, Hasan Gökçe *, İsmail Duman, M. Lütfi Öveçoğlu

Istanbul Technical University, Faculty of Chemical and Metallurgical Engineering, Department of Metallurgical and Materials Engineering, 34469 Maslak, Istanbul, Turkey

Available online 16 April 2011

Abstract

In this study, AlB_2 powders were synthesized by using a combined method of mechanical alloying (MA) and annealing of elemental aluminum (Al) and boron (B) powders. Milling was performed in a planetary ball-mill (Fritsch^{TM} Pulverisette 7 Premium Line) up to 15 h under argon (Ar) atmosphere. Annealing process was carried out in a tube furnace at 650 °C for 6 h under Ar atmosphere. The effects of MA durations on the annealing process and AlB_2 formation were investigated. The conversion of Al and B powders to AlB_2 starts after only MA for 3 h or after MA for 1 h and subsequent annealing. A slight formation of AlB_{12} occurs at 242 °C for as-blended powders and it shifts to about 272 °C for MA'd powders. Al–B powder blends MA'd for 9 h and annealed have AlB_2 particles in size between 35 and 75 nm in the presence of $Al_{13}Fe_4$, Fe_3B and Fe_2B contaminations.

Keywords: Powders-solid state reaction; Mechanical alloying; Boride; Thermal properties; X-ray methods

1. Introduction

The ternary alloy system Al–Ti–B has a great importance in aluminum industry as a grain refining agent for aluminum casting systems.[1–8] In recent years, several competitive cast aluminum metal matrix composites (MMC) belonging to this system have been fabricated.[1–12] When a mixture of boron and/or titanium and bearing salts are added into an Al-melt, TiB particles which behave as reinforcements in the Al-base matrix can be precipitated.[13,14] Similar to Ti, other transition metal impurities such as V, Cr and Zr can be readily precipitated and removed by C, since these transition borides are more stable than those of aluminum.[1–12] Thus, Al–B master alloys are used in the in situ fabrication of Al-matrix.[15–20] An example is the in situ fabrication of Al-AlB_2 metal composites using an Al–B master alloy.[21–25] The standard production of Al–B alloys requires the addition of KBF_4 salt into molten aluminum directly and is thus economical and practical.[16–20] Boron of the halide salt is reduced by aluminum and is dispersed into aluminum melt in the forms of aluminum borides AlB_2 and AlB_{12}. On the basis of the Al–B binary phase diagram shown in Fig. 1, AlB_{12} is a compound which forms at 975 °C as a result of the peritectic reaction. When AlB_{12} is cooled, it reacts with liquid aluminum to form AlB_2 (Liquid Al + α-AlB_{12} → AlB_2).[26,27] It is evident from Fig. 1 that AlB_{12} exists as a high temperature phase (>975 °C) at boron contents less than 44.5 wt.%. The presence of AlB_{12} at temperatures lower than 975 °C (peritectic temperature) is clearly indicated in Fig. 1 that AlB_{12} is stable at boron contents greater than 44.5 wt.% as a properitectic constituent. However, AlB_{12} is generally identified and seen in Al–B master alloys that have been obtained via reactions of molten salt at temperatures lower than the peritectic temperature.[16–22] The existence of AlB_{12} was indicated in Al–Ti–B master alloys that have been produced via arc melting process of aluminum and boron at 800 °C.[8–14]

Despite a number of studies on the AlB_2 formation by molten aluminum methods, there is no reported literature on the AlB_2

* Corresponding author at: I.T.U, Faculty of Chemical and Metallurgical Engineering, Department of Metallurgical and Materials Engineering, Ayazağa Campus, 34469 Maslak, Istanbul, Turkey. Tel.: +90 212 285 3090; fax: +90 212 285 3427.
E-mail addresses: bozkurtdu@itu.edu.tr (D. Ağaoğulları), gokceh@itu.edu.tr (H. Gökçe), iduman@itu.edu.tr (İ. Duman), ovecoglu@itu.edu.tr (M.L. Öveçoğlu).

0955-2219/$ – see front matter © 2011 Elsevier Ltd. All rights reserved.
doi:10.1016/j.jeurceramsoc.2011.03.037

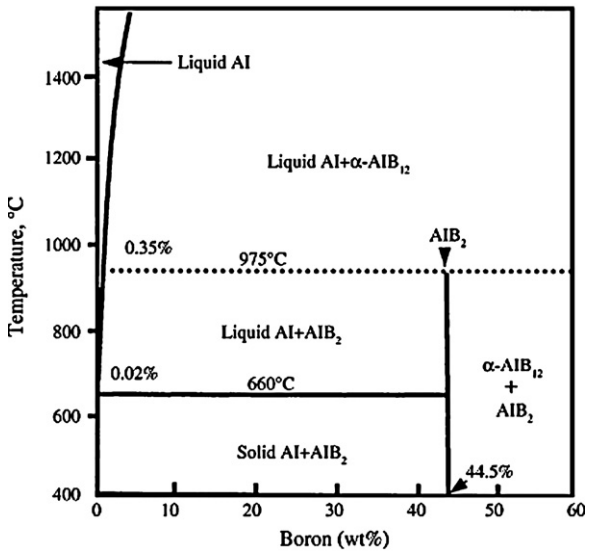

Fig. 1. Al–B binary phase diagram showing the AlB_2 line compound.[26,27]

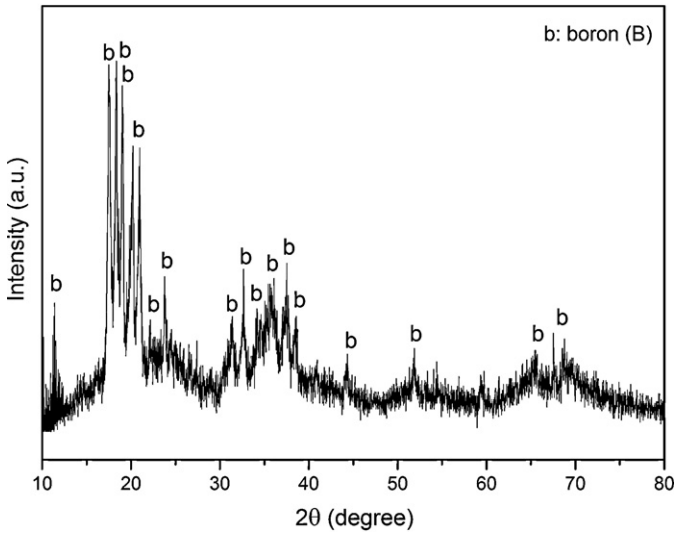

Fig. 2. XRD pattern of as-received boron powders.

synthesis by high energy ball milling (mechanical activation) techniques. In this respect, the present study will be the first to report on the AlB_2 powder synthesis. In the present study, AlB_2 powders were produced from Al–B elemental powders via mechanical activated annealing at 650 °C for 6 h. The effects of mechanical alloying duration on annealing process and formation of AlB_2 were evaluated.

2. Experimental procedure

Elemental aluminum (Al) powders (Alfa Aesar™, 99.5% purity, 12 μm average particle size), boron powders (commercial name: amorphous boron powders, Alfa Aesar™, 1 μm average particle size) were mixed to constitute the compositions of master alloy as Al-44.5 wt.% B. In each run, powder batches of 4 g were weighed in a Precisa™ XB320 M sensitive balance. In order not to cause any possible aluminum carbide formations during mechanical alloying, no process control agent (PCA) was added to each batch as to minimize cold welding between powder particles and thereby to inhibit agglomeration. Mechanical alloying (MA) experiments were carried out using a Frisch™ Pulverisette P7 Premium Line with a rotation speed of 1000 rpm in a hardened steel vial (45 ml) with hardened steel balls (ϕ 6 mm). Milling vials were evacuated to about 10^{-2} Pa and then sealed in a Plaslabs™ glove box under Ar gas (Linde™, 99.999% purity) to prevent surface oxidation and contamination of powder mixtures. Milling was performed using a ball-to-powder weight ratio (BPR) 10:1 in order to obtain large contact surfaces and fine pulverization. MA durations were varied from 1 h to 15 h. MA'd powders were unloaded again under Ar atmosphere in the glove-box. MA'd powders were annealed in a Thermo Scientific™ tube furnace for 6 h at 650 °C with a heating and cooling rate of 10 °C/min. under Ar gas flow rate of 2000 ml/min. As-blended (ab) and MA'd powder blends were heated in a TA™ Instruments Q600 differential scanning calorimeter (DSC) cell until 625 °C under flowing Ar gas at a heating rate of 10 °C/min. X-ray diffraction (XRD) investigations of the MA'd powders and MA'd/annealed powder samples were carried out using a Bruker™ D8 Advanced Series Powder Diffractometer with Cu Ka (1.54060 Å) radiation in the 2θ range of 10–100° with a step size of 0.02° at a rate of 1°/min. The International Center for Diffraction Data® (ICDD) powder diffraction files were utilized in the identification of crystalline phases. The average crystallite size and lattice strain of the MA'd powders were determined using a Bruker™-AXS TOPAS V3.0 software.[28] Furthermore, because of the exothermic peak at 242 °C observed in the DSC thermogram of the as-blended powder mixture, as-blended and MA'd powders were heated to 350 °C for 30 min. under flowing Ar gas in a tube furnace. These samples were rapidly cooled in Ar atmosphere to room temperature. Morphological characterizations of 9 h MA'd and annealed powders were conducted using a Jeol™-JEM-2000EX transmission electron microscope (TEM) operated at 160 kV.

3. Results and discussion

XRD investigations were carried out on boron powders, as-blended and MA'd Al–B powders. Fig. 2 is the XRD pattern taken from as-received boron powders, showing the presence of peaks belonging to (104), (0 2 1), (1 1 3), (2 0 2) and (0 1 5) reflections. Fig. 2 clearly indicates that boron powders used in this investigation are partially crystalline contrary to their commercial name 'amorphous boron'. Fig. 3(a) shows the XRD patterns of as-blended Al–B powders and those MA'd for 1, 3, 6, 9, 12 and 15 h. Fig. 3(b) is a blow-up portion of Fig. 3(a), presenting the XRD patterns of as-blended Al–B powders and this MA'd for 3 h in the 2θ interval between 15 and 25°. Characteristic peaks of Al which has a face-centered cubic Bravais lattice ($a = 0.405$ nm) are identified in the XRD patterns of as-blended and MA'd powders.[29] Reflections arising from boron which has a primitive rhombohedral Bravais lattice ($a = b = 1.095$ nm,

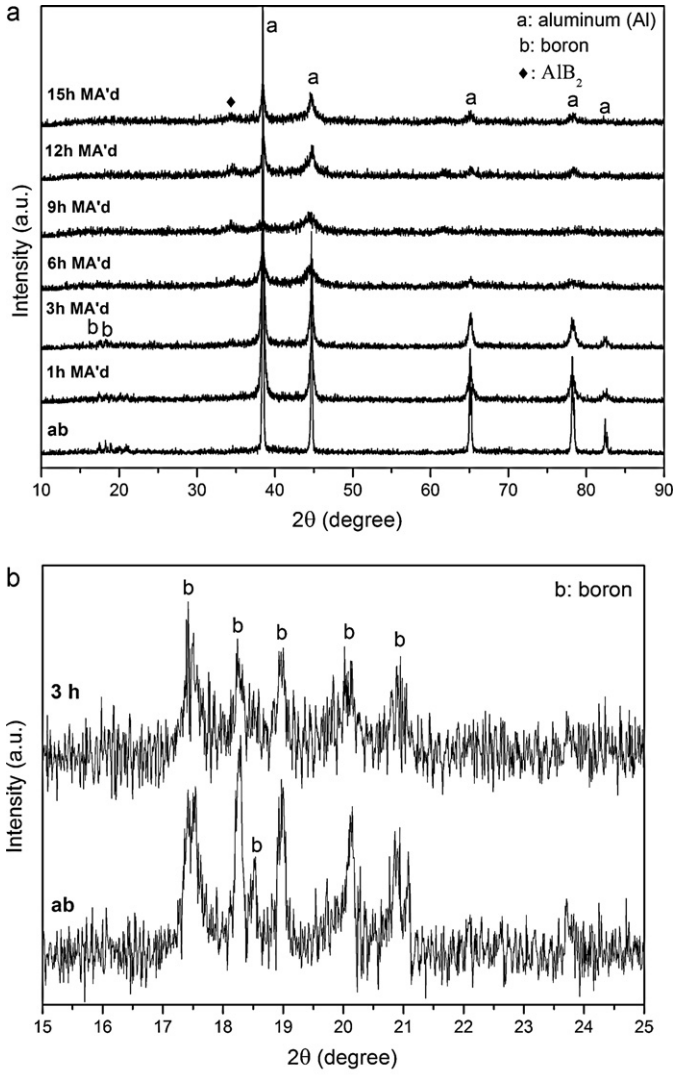

Fig. 3. (a) XRD patterns of the Al–B powder mixtures MA'd for different durations and (b) blow-up portion of the XRD patterns of as-blended Al–B powders and this MA'd for 3 h.

$c = 2.390$ nm) are also observed in the XRD patterns of as-blended powders and those MA'd for 1 and 3 h (Fig. 3a and 3b).[30] The disappearance of B peaks after MA for 6 h can be attributed to amorphization induced by MA process. A small reflection peak around $2\theta = 34^\circ$ emerges after MA for 3 h and its intensity increases with increasing milling time up to 12 h and it broadens after 15 h. The observed reflection peaks at $2\theta = 34.4^\circ$ in powders MA'd for 3–15 h belong to the (1 0 0) reflection of the AlB_2 phase which has a primitive hexagonal Bravais lattice ($a = b = 0.301$ nm, $c = 0.325$ nm).[31] Thus, due to the reactions between Al and B, a slight formation of the AlB_2 phase takes place during milling process after 3 h.

Furthermore, Fig. 3(a) indicates the broadening of Al peaks with prolonging milling durations. Continuous deformation of powders during milling results in crystallite refinement and increase in lattice strain. Table 1 represents the average crystallite size and lattice strain of Al particles in Al–B powder mixtures MA'd until 6 h. The average crystallite size of Al decreases from 238 nm to about 14.8 nm. In contrast to crystallite size, lattice strain increases up to 0.0537 with extended MA durations.

Table 1
The average crystallite size and lattice strain of as-blended Al–B powder mixtures and those MA'd for different durations.

BPR	Milling Duration	Crystallite size (nm)	Lattice strain
10/1	0	238	0.00
	1	60	0.03840
	3	33.1	0.04674
	6	14.8	0.05370

Since MA is a non-equilibrium high energy milling process, powders fabricated by this technique can undergo several microstructural and/or phase transformations during heating. In order to study possible microstructural changes and thermal stability of the Al–B powders, differential scanning calorimetry

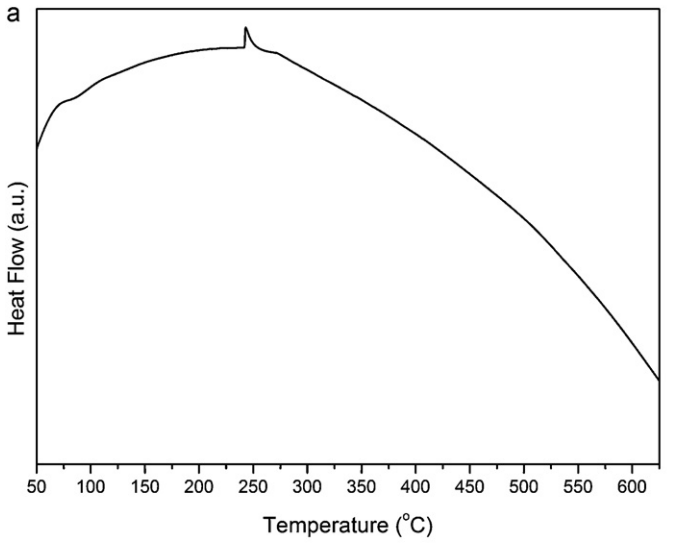

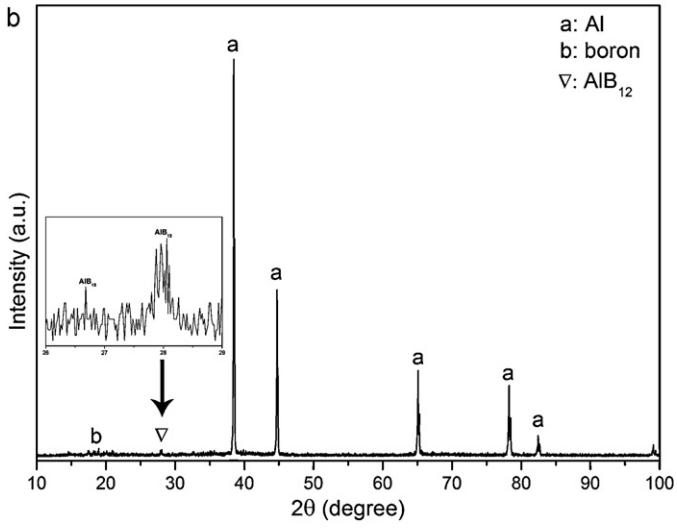

Fig. 4. (a) DSC thermogram of the as-blended Al–B powder and (b) XRD pattern of the as-blended Al–B powder annealed at 350 °C.

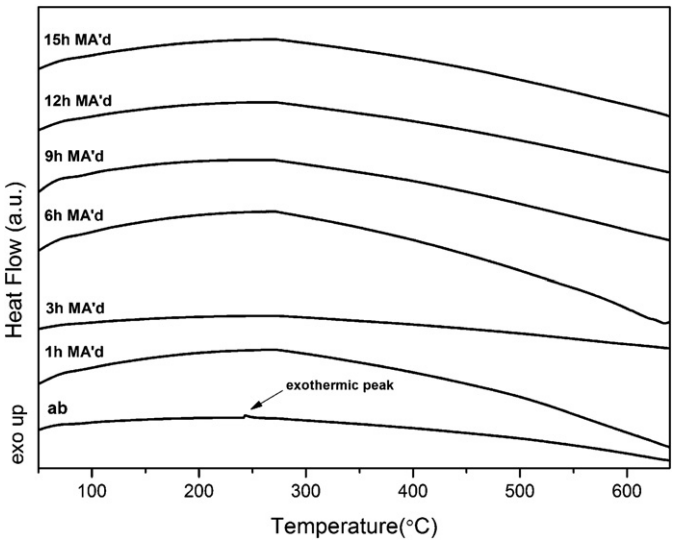

Fig. 5. DSC thermograms of as-blended and MA'd Al–B powder mixtures.

(DSC) analyses were carried out up to 625 °C. First of all, as-blended Al–B powders were chosen for the thermal analysis, as seen in Fig. 4(a). DSC thermogram of as-blended Al–B powder indicates a clear and sharp exothermic peak at 242 °C. In order to determine a new phase resulting from the exothermic peak, a XRD investigation was carried out on the as-blended Al–B powder (Fig. 4b) which was annealed at 350 °C (above the peak temperature in Fig. 4a) for 30 min. Presence of the Al and B phases and the incubation of the AlB_{12} phase which has a primitive tetragonal Bravais lattice ($a = b = 1.015$ nm, $c = 1.429$ nm) are clearly seen in Fig. 4(b).[32] Secondly, DSC analyses were conducted on all MA'd powders, as shown in Fig. 5. Similar to the DSC thermogram of as-blended powder, all MA'd powders have only small exothermic peaks. However, the temperatures of the exothermic peaks shift from 242 °C to about 272 °C (peak temperature) for all MA durations. On the basis of Figs. 4(a) and (b), and 5, all MA'd powder samples were annealed at 350 °C. XRD patterns of these samples reveal only Al, B and AlB_{12} phases and the AlB_2 phase was not observed. For this reason, a higher annealing temperature of 650 °C was chosen.

Fig. 6 shows the XRD patterns of Al–B powders MA'd for different durations (up to 15 h) and annealed at 650 °C for 6 h. As seen in Fig. 6, as-blended and annealed powders have AlB_2 phase in the presence of Al. All powders MA'd at durations between 1 h and 15 h comprise the AlB_2 phase and a very small amount of Al. The peaks of AlB_2 at about 45° and 62° broaden as MA duration increases from 1 to 15 h indicating the formation of AlB_2 in smaller crystallite sizes. In addition, $Al_{13}Fe_4$ phase which has a base-centered orthorhombic Bravais lattice ($a = 0.775$ nm, $b = 0.404$ nm, $c = 2.377$ nm)[33] and Fe_3B which has a primitive orthorhombic Bravais lattice ($a = 0.673$ nm, $b = 0.433$ nm, $c = 0.547$ nm)[34] are identified in all annealed samples. It is quite certain that $Al_{13}Fe_4$ and Fe_3B phases result from the Fe contamination by the milling media.

On the basis of the XRD patterns shown in Fig. 6, the main reactions occurred during annealing which resulted in the formation of the AlB_2 phase are in accordance with the phase transformations observed during DSC experiments. Since powder blends have the stoichiometric amounts of Al and B powders to form AlB_2, it is unexpected to obtain the AlB_{12} phase. However, an annealing temperature of 350 °C is not enough to grow stable AlB_2 phase, as obviously seen in Fig. 4(a) and (b). Annealing at 650 °C for 6 h provides AlB_{12} transformation to AlB_2, since the annealing temperature of 650 °C is very close to the melting point of Al. Although there was no indication for the formation of $Al_{13}Fe_4$ and Fe_3B phases in the DSC thermograms of the MA'd powders (Fig. 5), annealing for 6 h causes them to emerge in the XRD spectra (Fig. 6). Therefore, the reactions which take place during annealing led to the formation of the AlB_2 main stable phase and also $Al_{13}Fe_4$ and Fe_3B intermetallics.

Fig. 7(a), (b) and (c) shows the TEM micrographs (bright-field-BF, dark-field-DF and selected area diffraction pattern-SADP, respectively) taken from an agglomerate of the Al–B powders MA'd for 9 h and annealed at 650 °C for 6 h, revealing the presence of AlB_2 particles ranging in size between 35 and 75 nm. Fig. 8(a), (b) and (c) illustrates the TEM micrographs (BF, DF and SADP, respectively) taken from a different region in the Al–B powders MA'd for 9 h and annealed at 650 °C for 6 h, showing spherical/spheroidal Fe_2B particles ranging in size between 10 and 50 nm. Although XRD patterns of the MA'd and annealed powders shown in Fig. 6 indicate the presence of Fe_3B, TEM characterizations revealed Fe_2B as a new phase resulting from contamination. In overall, AlB_2 powder was synthesized from Al–B powder blends using a combined technique of mechanical alloying and annealing. In order to obtain pure AlB_2 powders in the absence of $Al_{13}Fe_4$ and Fe_3B phases, physical and/or chemical seperation techniques should be utilized which are beyond the scope of this investigation.

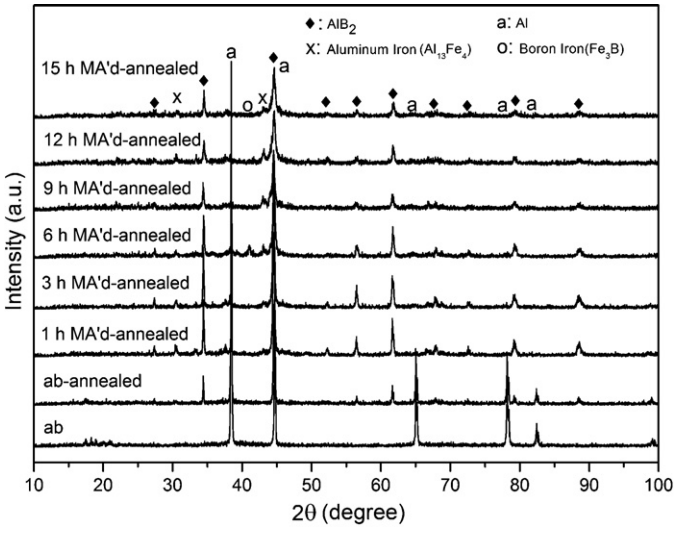

Fig. 6. XRD patterns of Al–B powder mixtures MA'd and annealed at 650 °C for 6 h.

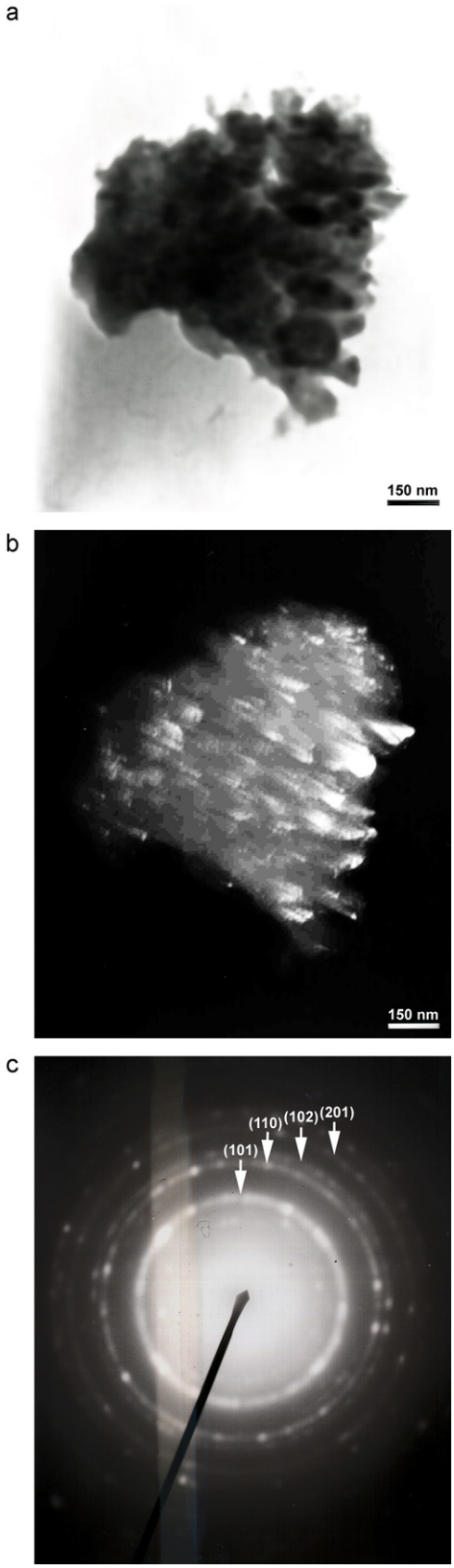

Fig. 7. TEM micrographs taken from an agglomerate of Al–B powders MA'd for 9 h and annealed at 650 °C for 6 h: (a) Bright-field image, (b) dark-field image, and (c) selected area diffraction pattern revealing the presence of AlB_2 particles ranging in size between 35 and 75 nm. Objective aperture is on (1 0 1) and camera length is 100 cm.

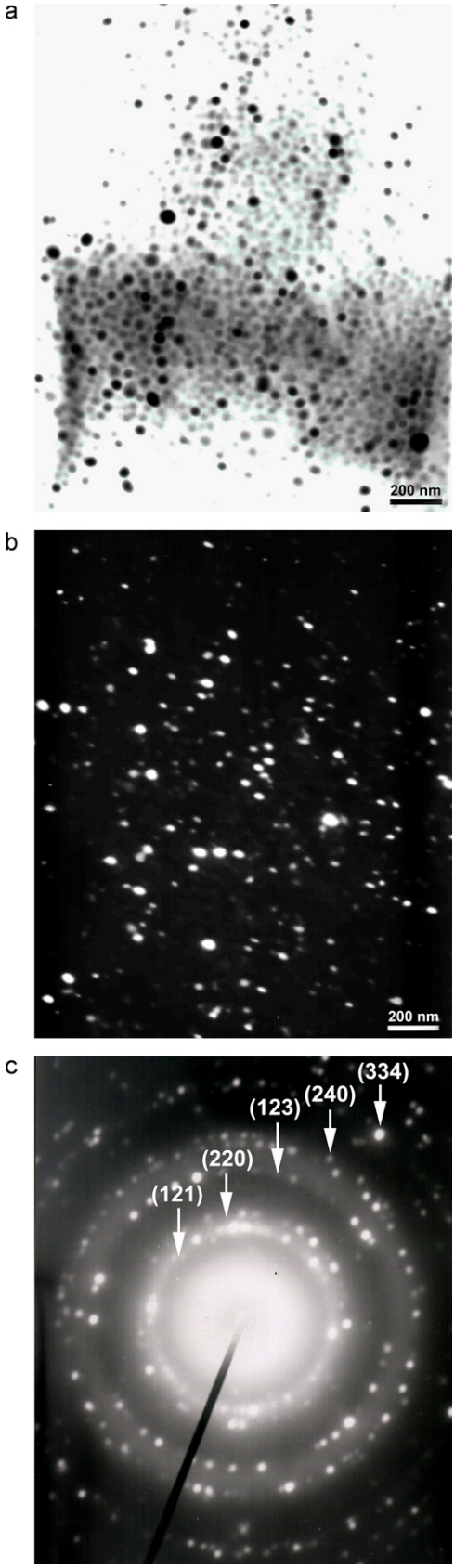

Fig. 8. TEM micrographs taken from Al–B powders MA'd for 9 h and annealed at 650 °C for 6 h: (a) Bright-field image, (b) dark-field image and (c) selected area diffraction pattern revealing the presence of spherical/spheroidal Fe_2B particles ranging in size between 10 and 50 nm. Objective aperture is on (1 2 1) and camera length is 100 cm.

4. Conclusions

Considering the results obtained in the present study, the following conclusions can be stated:

1. XRD investigations in the as-blended and MA'd Al–B powders reveal that Al and B peaks are present after MA for 15 h in the presence of AlB_2 which emerges after MA for 3 h.
2. Extending the MA duration results in decrease in the crystallite sizes of Al and also AlB_2 powders obtained after annealing.
3. On the basis of DSC experiments conducted up to 625 °C, as-blended and MA'd powders show exothermic peaks at the temperatures between 242 and 272 °C since they have a highly deformed structure after MA process. The exothermic peaks arise from the reaction between Al and B to form the AlB_{12} phase.
4. XRD patterns reveal that stable AlB_2 phase and $Al_{13}Fe_4$ and Fe_3B intermetallics due to contamination are present in each sample after annealing at 650 °C for 6 h.
5. TEM characterizations prove the presence of AlB_2 particles ranging in size between 35 and 75 nm. Also, Fe_2B particles ranging in size between 10 and 50 nm were observed which could not be detected in XRD analyses.

Acknowledgements

The authors would like to express their appreciations to Aziz Genç for his help in TEM experiments. We would like to express our gratitude to State Planning Organization (DPT) for funding the projects entitled "Advanced Technologies in Engineering" with the project number 2001K120750 and "Development of Al–Cu Based Metal Matrix Composites via Powder Metallurgy Techniques" with the project number 90189 out of which the main infrastructure of the Particulate Materials Laboratories was founded.

References

1. Chu MG. Microstructure solidification analysis of melt-spun Al–Ti and Al–Ti–B. *Materials Science alloys Engineering: A* 1994;**179–180**:669–752.
2. Kumar V, Murty GS, Chakraborty BS. Grain refinement response of LM25 alloy towards Al–Ti–C and Al–Ti–B grain refiners. *Journal of Alloys and Compounds* 2009;**472**:112–20.
3. Murty GS, Kori SA, Venkateswarlu K, Bhat RR, Chakraborty M. Manufacture of Al–Ti–B master alloys by the reaction of complex halide salts with molten aluminium. *Journal of Materials Processing Technology* 1999;**89–90**:152–8.
4. Nikitin VI, Wanqi JIE, Kandalova EG, Makarenko AG, Yong L. Preparation of Al–Ti–B grain refiner by SHS technology. *Scripta Materialia* 2000;**42**:561–6.
5. Peijie L, Kandalova EG, Nikitin VI, Luts AR, Makarenko AG, Zhang Y. Effect of fluxes on structure formation of SHS Al–Ti–B grain refiner. *Materials Letters* 2003;**57**:174–9.
6. Birol Y. Production of Al–Ti–B grain refining master alloys from $Na_2B_4O_7$ and K_2TiF_6. *Journal of Alloys and Compounds* 2008;**458**:271–6.
7. Limmaneevichitr C, Eidhed W. Novel technique for grain refinement in aluminum casting by Al–Ti–B powder injection. *Materials Science Engineering A* 2003;**355**:3694–8.
8. Birol Y. A novel Al–Ti–B alloy for grain refining Al–Si foundry alloys. *Journal of Alloys and Compounds* 2009;**486**:219–22.
9. Birol Y. Al–Ti–B grain refiners via powder metallurgy processing of $Al/K_2TiF_6/KBF_4$ powder blends. *Journal of Alloys and Compounds* 2009;**480**:311–4.
10. Birol Y. An improved practice to manufacture Al–Ti–B master alloys by reacting halide salts with molten aluminium. *Journal of Alloys and Compounds* 2006;**420**:71–6.
11. Birol Y. Production of Al–Ti–B grain refining master alloys from B_2O_3 and K_2TiF_6. *Journal of Alloys and Compounds* 2007;**443**:94–8.
12. Fjellstedt J, Jarfors AEW, Svendsen L. Experimental analysis of the intermediary phases AlB_2, AlB_{12} and TiB_2 in the Al–B and Al–Ti–B systems. *Journal of Alloys and Compounds* 1999;**283**:192–7.
13. Lu L, Lai MO, Wang HY. Synthesis of titanium diboride TiB_2 and Ti–Al–B metal matrix composites. *Journal of Materials Science* 2000;**35**: 241–8.
14. Lee MS, Terry BS, Grieveson P. Interfacial phenomena in the reactions of Al–B, Al–Ti–B and Al–Zr–B alloys with KF-AlF_3 and NaF-AlF_3 melts. *Metallurgical Materials Transactions B* 1993;**24**:947–53.
15. Fjellstedt J, Jarfors AEW, El-Benawy T. Experimental investigation and thermodynamic assessment of the Al-rich side of the Al–B system. *Materials & Design* 2001;**22**:443–9.
16. Birol Y. Production of Al–B alloy by heating Al/KBF_4 powder blends. *Journal of Alloys and Compounds* 2009;**481**:195–8.
17. Wang X. The formation of AlB_2 in an Al–B master alloy. *Journal of Alloys and Compounds* 2005;**403**:283–328.
18. Samsonov GV, Neronov VA, Lamikhov LK. The conditions, structure and some properties of phases in the Al–B system. *Journal of the Less Common Metals* 1979;**67**:291–6.
19. Van Setten MJ, Fichtner M. On the enthalpy of formation of aluminum diboride, AlB_2. *Journal of Alloys and Compounds* 2009;**477**: L11–2.
20. Mirkovic D, Gröbner J, Schmid-Fetzer R, Fabrichnaya O, Lukas HL. Experimental study and thermodynamic re-assessment of the Al–B system. *Journal of Alloys and Compounds* 2004;**384**:168–74.
21. Ma ZY, Tjong SC. In situ ceramic particle-reinforced aluminum matrix composites fabricated by reaction pressing in the TiO_2 (Ti)–Al–B (B_2O_3) systems. *Metallurgical Materials Transactions A* 1997;**28**: 1931–42.
22. Deppisch C, Liu G, Shang JK, Economy J. Processing mechanical properties of AlB_2 flake reinforced Al-alloy composites. *Materials Science Engineering A* 1997;**225**:153–61.
23. Kubota M, Kaneko J, Sugamata M. Properties of mechanically milled spark plasma sintered Al–AlB_2 and Al–MgB_2 nano-composite materials. *Materials Science Engineering: A* 2008;**475**:96–100.
24. Melgarejo ZH, Resto PJ, Stone DS, Suárez OM. Study of particle–matrix interaction in Al/AlB_2 composite via nanoindentation. *Materials Characterization* 2010;**61**:135–40.
25. Jackson MJ, Graham ID. Mechanical stirring of Al–B alloys. *Journal of Materials Science Letters* 1994;**13**:754–6.
26. Duschanek H, Rogl P. The Al–B (aluminum–boron) system. *Journal of Phase Equilibria* 1994;**15**:543–52.
27. Okamoto H. Al–B (aluminum–boron). *Journal of Phase Equilibria and Diffusion* 2006;**27**:195–6.
28. Kern AA, Coelho AA. *Bruker-AXS TOPAS V. 3.0*; 2006. www.brukeraxs.com.
29. Powder Diffraction Files: Card No 04-0787, database edition, The International Center for Diffraction Data (ICDD).
30. Powder Diffraction Files: Card No. 85-0409, database edition, The International Center for Diffraction Data (ICDD).
31. Powder Diffraction Files: Card No. 39-1483, database edition, The International Center for Diffraction Data (ICDD).
32. Powder Diffraction Files: Card No. 16-0278, database edition, The International Center for Diffraction Data (ICDD).
33. Powder Diffraction Files: Card No. 50-0797, database edition, The International Center for Diffraction Data (ICDD).
34. Powder Diffraction Files: Card No. 35-1339, database edition, The International Center for Diffraction Data (ICDD).